Research Article | Vol. 27, No. 18 | 2 Sep 2019 | OPTICS EXPRESS 25493
Optics EXPRESS

A general model for taper coupling of multiple modes of whispering gallery resonators and application to analysis of coupling-induced Fano interference in a single cavity

SHAHAB BAKHTIARI GORAJOOBI,* GANAPATHY SENTHIL MURUGAN, AND MICHALIS N. ZERVAS

Optoelectronics Research Centre, University of Southampton, Southampton, SO17 1BJ, UK
sbg1v17@soton.ac.uk

Abstract: In this paper, we give a general model for analysis of multimode Whispering Gallery Mode (WGM) resonators coupled to multimode tapered fibers based on the coupled-mode theory. Such formulation takes into account the asymmetry of the taper-resonator coupling. Simulations for a microsphere show that the tapered fiber coupling mechanism induces cross-coupling between coherent orthonormal WGMs. We show that the degree of such cross-coupling depends basically on the fiber diameter, air-gap between the taper and resonator, intrinsic losses and eccentricity. The WGM cross-coupling affects the total transmission and spectral line-shape of the internal powers resulting in a controllable transformation of the line-shape to non-Lorentzian spectra. This analysis can be utilized to precisely determine the output and intra-cavity intensity of multimode microresonators, which is important in lasers, nonlinear optical signal generation and realization of optical delays.

1. Introduction

The transmission spectrum of a Waveguide-coupled optical Whispering Gallery Mode (WGM) microresonator is a result of interference between the incoming waveguide-mode and the out-coupled excited resonator-modes. Due to ultra-high Quality (Q) factor and easy fabrication, spherical resonators have been extensively employed for realization of lasers, filters, nonlinear devices, cavity-atom systems and sensors [1–4]. In most cases, the WGM excitation/collection is achieved through tapered fibers owing to their high efficiency, compatibility with the current optical technologies and availability [5,6]. Nearly, all the 3D WGM resonators exhibit multimodal operation, which although in some cases induces problems such as instability in lasers, it leads to interesting optical phenomena. Coherent interference of a specific WGM with another resonant mode with different bandwidth results in alteration of the transmission spectrum to a non-Lorentzian line-shape by virtue of Fano interference. In fact, such interference is a result of interaction of fields with different pathways which can be experimentally realized in coupled [7] or single cavities [8, 9]. In both such configurations (i.e. coupled and single cavities), two distinct uncoupled WGMs are mutually coupled through either direct cavity-coupling or indirect taper-coupling mechanisms.

Despite the wide application of taper-coupled coherent multimode WGM resonators there have been limited studies considering the effects of the tapered fiber on excitation of WGMs in a single cavity. Most of the the theoretical works focus on only two-mode interference and do not explain the multi-modal coupling process from which the important Fano interferences stem. However, three-mode interference has been experimentally demonstrated in microbottle resonators [10]. In addition, such analyses do not generally incorporate the asymmetry of the taper-resonator coupling which is important in accurately-estimating the out-coupling loss (i.e. Q factor), and

#369053 https://doi.org/10.1364/OE.27.025493
Journal © 2019 Received 5 Jun 2019; revised 26 Jul 2019; accepted 29 Jul 2019; published 23 Aug 2019

Optics EXPRESS

becomes an issue in the strong coupling regimes due to violation of power conservation. In this letter, using the well-known Coupled-Mode Theory (CMT) for asymmetric coupled waveguides, we derive a general classical model describing the transmission of a multimode microresonator coupled to a multimode tapered fiber in a systematic fashion. The model is then applied to a silica microsphere exhibiting degenerate WGMs resembling a coherent multimode cavity, and it is demonstrated that depending on the tapered fiber loading, WGMs contribute to the distortion of the total transmission spectra of the resonator to a non-Lorentzian line-shape.

2. Derivation of the resonator-taper coupled-mode equations

In order to evaluate the total transmission of the taper-microsphere system, we adopt the well-known CMT [11, 12]. Let us assume all the modes propagating along the coupler illustrated in Fig. 1(a) as a vector denoted by $a(z) = [\ a_f(z)^t \quad a_1(z) \quad a_2(z) \quad \dots \quad a_N(z)\ ]^t$ where $a_f(z) = [\ a_{f1}(z) \quad a_{f2}(z) \quad \dots \quad a_{fP}(z)\ ]^t$ and $a_i(z)$ (with $1 \leqslant i \leqslant N$) are respectively the electric field amplitude of the P considered fiber modes and WGM with order i at position z. Then, the CMT formulation for the coupling region is given by $da(z)/dz = jM(z)a(z)$ where $M = B + C^{-1}K$ represents an effective coupling matrix, and B denotes the diagonal propagation constant matrix given as $B = diag(\beta_{f1},\dots,\beta_{fP},\beta_1,\dots,\beta_N)$ where β signifies the propagation constant and subscripts indicate either fiber ($f1 - fP$) or WGMs ($0 - N$). Elements of matrices K and C at an air-gap of S are given by $K_{ij}(S) = k^2(2\beta_i)^{-1}\iint(n_i{}^2 - n_0{}^2)E_i{}^*.E_j dxdy$ and $C_{ij}(S) = \iint E_i{}^*.E_j dxdy$ for which the integrals are taken on guide i and all space, respectively. k, n_i and n_0 are the wave-number, refractive indices of guide i and air, respectively. Here, K_{ij} is the coupling coefficient of mode j with normalized electric field (i.e. having power of 1W) of E_j to mode i with normalized electric field of E_i. i and j can be any fiber or WGMs. It should be noted that, in a microsphere eigenmodes are orthonormal (i.e. $C_{ii} = 1$), hence, coupling coefficients between distinct WGMs are zero, and generally $K_{ij} \neq K_{ji}$ (for $i \neq j$) while $C_{ij} = C_{ji}$. The solution of the CMT equation is given by $b(z) = \exp\{jM(z)\}a(0)$ where $a(0)$ is the initial value, and $b(z) = [\ b_f(z)^t \quad b_1(z) \quad b_2(z) \quad \dots \quad b_N(z)\ ]^t$. Here, $b_f(z) = [\ b_{f1}(z) \quad b_{f2}(z) \quad \dots \quad b_{fP}(z)\ ]^t$ is a vector representing the solution for the fiber modes. Value of $\exp\{jM(z)\}$ can be evaluated from the eigenvalue solutions of matrix M.

The coupled-mode solution can be calculated for each section of the coupler tapered into $N_c + 1$ consecutive small directional couplers with length of Δz and fixed separation of S_i (where $-N_c/2 \leqslant i \leqslant N_c/2$, and N_c even) from the fiber center (as demonstrated in Fig. 1(a)). Thus, the total transfer matrix of the coupler is $\Lambda = \prod_{i=0}^{Nc}\exp\{jM_{(-N_c/2+i)}\Delta z\}$. Let us signify the internal amplitudes of the resonator WGMs at the beginning and end of the coupler region by $a_{wgm}(0) = [\ a_1(0) \quad a_2(0) \quad \dots \quad a_N(0)\ ]^t$ and $b_{wgm}(L_c) =$

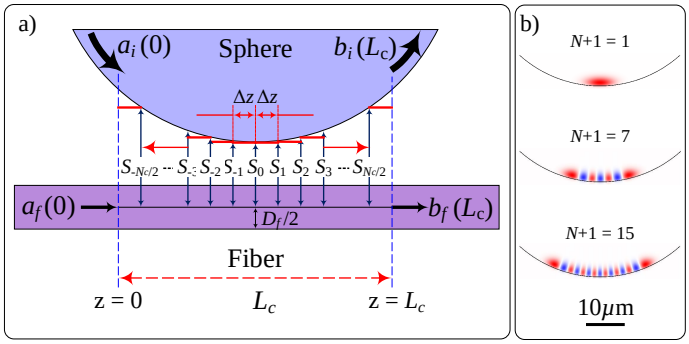

Fig. 1. a) Schematic of the taper-coupled microresonator system showing the inputs and outputs of the coupling region, and b) typical calculated electric of the 1st, 7th and 15th order WGMs with radial order of one for a silica microsphere with radius of 30μm.

Optics EXPRESS

$[\ b_1(L_c)\quad b_2(L_c)\quad \ldots\quad b_N(L_c)\ ]^t$, respectively. $a_{wgm}(0)$ and $b_{wgm}(L_c)$ are related through the propagation of WGMs in the resonator, given by a diagonal transformation matrix T_F such that $a_{wgm}(0) = T_F b_{wgm}(L_c)$ where $T_F = diag(T_{FB(1)}, T_{FB(2)}, \ldots, T_{FB(N)})$. Each round-trip transformation element is given by $T_{FB(i)} = \exp\{(2\pi R_0 - L_c)\alpha_{\text{int}(i)} + j\varphi_{rt(i)}\}$ where $\alpha_{int(i)}$ is the total intrinsic loss parameter (including scattering, material and absorption losses per unit of length) of mode i with effective refractive index of $n_{eff(i)}$ at wavelength of λ_i and given in terms of Q-factor ($Q_{\text{int}(i)}$) by $\alpha_{\text{int}(i)} = 2\pi n_{eff(i)}/Q_{\text{int}(i)}\lambda_i$. The round-trip phase shift, $\varphi_{rt(i)}$, can be calculated from the modified resonance condition for mode i such that $\varphi_{rt(i)} + \Delta\varphi_{c(i)} = 2\pi m$ where m is the azimuthal mode number and the coupler-induced phase-shift on mode i is calculated from the diagonals of transfer matrix of the coupler by $\Delta\varphi_{c(i)} = \angle\Lambda_{ii}$. For simplicity, let us define matrices V_1, V_2, V_3 and V_4 from Λ such that

$$\Lambda = \left[\Lambda_{ij}\right]_{(N+P)\times(N+P)} = \begin{bmatrix} [V_1]_{P\times P} & [V_2]_{P\times N} \\ [V_3]_{N\times P} & [V_4]_{N\times N} \end{bmatrix} \tag{1}$$

and write the input-output coupler relation in the form of $[\ b_f(L_c)^t\quad b_{wgm}(L_c)^t\ ]^t = \Lambda[\ a_f(0)^t\quad a_{wgm}(0)^t\ ]^t$. Then, by simple matrix manipulations, the output of the tapered fiber modes, $b_f(L_c)$, and the internal field amplitudes, $a_{wgm}(0)$, can be written as a function of the input fiber modes, $a_f(0)$, such that $a_{wgm}(0) = [({T_F}^{-1} - V_4)^{-1}V_3]a_f(0)$ and $b_f(L_c) = [V_1 a_f(0) + V_2 a_{wgm}(0)]$. It should be noted that, in the course of this work, we consider only the fundamental linearly-polarized mode (LP_{01}) of the fiber for the sake of the simplicity. However, such formulation is generic and can be easily applied to a multi-input-multi-output system.

3. Simulation results

3.1. Effects of taper and resonator air-gap

We consider an ideal silica microsphere surrounded by air with a radius of 30μm and refractive index of 1.45. The spherical and tapered fiber modes can be calculated from the analytical characteristics and field relations given in [13]. Figure 1(b) exemplifies field distribution of few

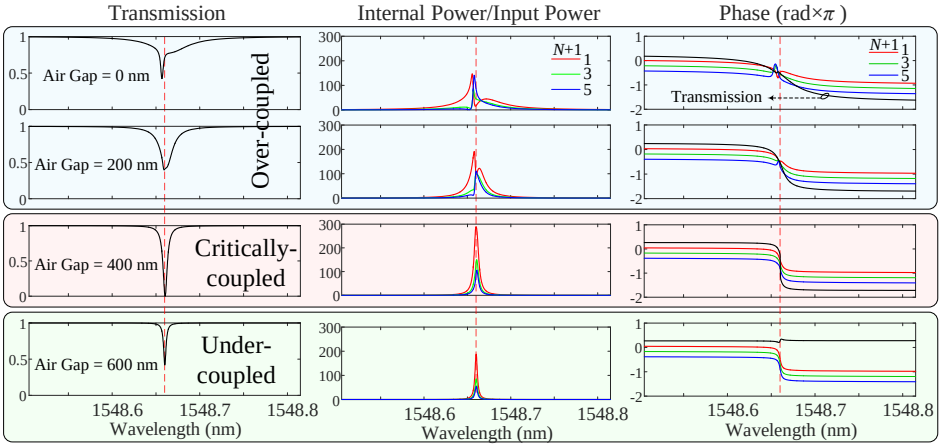

Fig. 2. Spectra of transmission, internal power enhancement and internal WGM phase of tapered fiber coupled microsphere considering degenerate modes of 1st, 3rd and 5th orders as a function of fiber-to-sphere air-gap. The intrinsic Q of all modes is set to 10^6 and the tapered fiber diameter is 2μm (dashed lines show the position of the isolated microsphere resonance wavelength).

Optics EXPRESS

calculated WGMs with $N+1 = 1, 7, 15$ where N is the order of the Hermite polynomials in the angular component of the spherical field and $N+1$ is equal to the number of field extrema in the angular direction. Figure 2 shows the calculated transmission, internal/output power ratio and phase (of internal WGMs $a_i(0)/a_f(0)$, and transmission $b_f(L_c)/a_f(0)$) spectra of the system for a taper diameter of $D_f = 2\mu$m as function of the air-gap between the taper and microsphere. The intrinsic Q of the WGMs is considered to be 10^6 , and for the sake of simplicity, only the first five degenerate modes ($N = 0-4$) of the first radial order at 1548.66nm are considered. Even ($N+1$) mode orders are not plotted due to zero coupling coefficient to such WGMs. The simulations show that, at very small air-gaps, symmetric Lorentzian shape of the transmission spectrum is distorted. The internal-to-input-power ratios of WGMs at zero air-gap show a Fano-like line shape. The phase spectra of the internal modes show that, at very small air-gaps where there is strong coupling with the fiber mode, coupling-induced phase variations of individual modes increase. Consequently, the phase of the total transmission shows a non-monotonic transition as the wavelength increases. Accordingly, the dip of the power transmission spectrum shows a slight frequency shift with respect to the uncoupled resonator resonance frequency as a result of the pronounced mode interference. On the other hand, as the air-gap between the taper and microsphere increases, phase perturbations due to effect of the fiber coupling on WGMs, progressively diminish. Subsequently, the transmission spectrum becomes closer to a Lorentzian line shape. At air-gaps larger than 300nm, the fundamental WGM is dominantly excited owing to its higher total Q factor comparing to small air-gaps, as well as greater modal overlap compared to the higher order WGMs. Hence, the effect of the higher order WGMs on the total output field is not anymore significant resembling a weakly-driven cavity. The resonator exhibits critical-coupling at air-gap of 400nm below and above which transmission is non-zero due to over- and under-coupling, respectively. Additionally, excited WGMs show degenerate frequency responses by widening the air-gap. Such analyses are important as they show within a variation of 200nm from the critical-coupling air-gap, the internal power of the fundamental WGM drops to $\sim 2/3$ of the critical value. This can be extended to study the control precision required for maintaining a certain internal power in a particular application. Such control precision is, of course, dependent on the intrinsic Q of the WGMs.

The resonance condition implies that the resonance frequency of a particular WGM is always set to the uncoupled cavity resonance frequency. In other words, the round-trip phase shift is

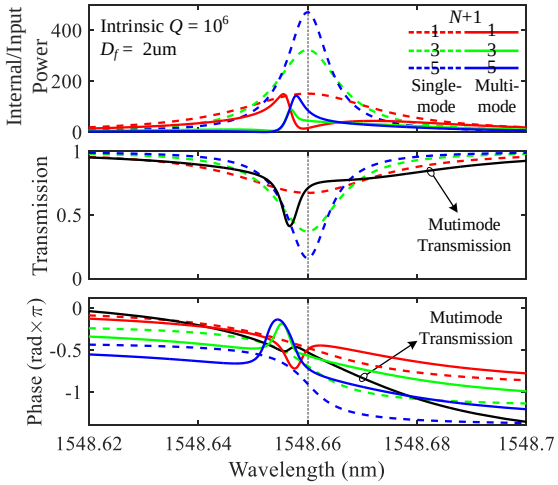

Fig. 3. Internal power enhancement, transmission and phase spectra of tapered fiber-coupled microsphere with zero air-gap, taper diameter of 2μm and intrinsic Q of 10^6. Results are shown for WGMs with $N+1 = 1$, 3 and 5 when the cavity operates in single-mode (dashed lines) or multimode (solid lines) regimes.

Optics EXPRESS

always compensated by the effect of fiber-coupling induced phase shift. Cavity index-perturbation due to coupler is experimentally shown to shift the cavity resonance depending on the air-gap between the excitation coupler (e.g. tapered fiber, waveguide, etc.) and the resonator, as well as, relative sizes of the resonator and the coupler [14–17]. In contrast, the complicated transmission spectra of the current analysis is only owing to the modal interference between coherent WGMs due to the coupling system. It should be noted that, solving the coupled equations for the asymmetric taper-microsphere coupler, generally, results in an asymmetric matrix Λ, with nonzero off-diagonal elements. The first row and column show the coupling between fiber and WGMs, while the rest of the off-diagonal elements correspond to energy transfer between WGMs due to the coupler perturbation. Note that, intera-cavity whispering gallery modal-coupling due to cavity index imperfections can be also easily incorporated once the coupling coefficients are known. Such energy transfers will be manifested in the appropriate (i.e. excluding first row and column) off-diagonal elements of Λ.

Figure 3 shows simulations for the microsphere coupled to a taper with 2μm diameter at zero air-gap. The results are shown for both cases when cavity operates in single-mode or multimode conditions. The multimode transmission of the resonator shows the effects of modal cross-coupling between the WGMs in presence of fiber coupling. The response of each isolated WGM shows a generic Lorentzian line shape with a monotonic phase shift around the resonance frequency. In the presence of simultaneous excitation of degenerate (coherent) WGMs, phases of the internal mode amplitudes change non-monotonically, and are affected by the amount of WGM cross-couplings. Such interference between the modes deforms the internal power variation to a Fano-like shape. Note that, the relative phases between the WGMs are determined by the coupling region, and vary depending on the amount of their phase-mismatch and overlap with the fiber mode. Certainly, changing the resonator size will alter such amounts and the coupling regime under which each WGM operates.

3.2. *Effects of intrinsic and extrinsic (taper-induced) losses*

Moreover, the modal interference between the degenerate WGMs depends on the coupling condition under which each mode is excited. Figure 4 plots the transmission and amount of internal power enhancement when the intrinsic Q of the cavity is varied for fixed taper diameter and air-gap values of 2μm and zero, respectively. For very low intrinsic Q's (i.e. 5×10^4) most of the modes are under-coupled, hence, the dominant excited mode corresponds to the fundamental mode (which is close to critical-coupling) owing to its high overlap with the fiber mode. As the intrinsic Q factor gradually increases, the fundamental mode is over-coupled and the higher order modes reach critical-coupling condition. The relatively higher internal power of high order WGMs increases the modal interference between the modes. At very high intrinsic Q's (i.e. 1×10^8), WGMs get into over-coupling regime. Note that, we considered similar intrinsic Q's for WGMs as they belong to the same cavity. Thus, such line-shapes are outcomes of resonances with slightly different bandwidths due to the taper loading. In [18],two cavities (i.e. disk and toroid) with very dissimilar Q's (i.e. resonance bandwidths) are coupled through a tapered fiber. Hence, a discernible asymmetric Fano resonance is observed. Similar transmission spectra to Fig. 4 are observed for a hollow microbottle resonator when the interaction of two WGMs is tuned in frequency by the inner pressure of the resonator [19]. Furthermore, cross-coupling between degenerate WGMs depend on the fiber diameter, as it determines the amount of fiber mode coupling and phase-matching to WGMs. Figure 5 shows the results when the taper diameter is varied between 1.2μm and 9.2μm at a fixed air gap of zero and intrinsic Q of 10^6. At very small taper diameters (i.e. 1.2μm), WGMs are over-coupled due to high modal overlap between the fiber and WGMs. Despite the close-to-90% transmission of the system at $D_f = 1.2\mu m$, the internal powers of WGMs are not significantly dampened compared to the cases where the transmission is very low. The cross-coupling between WGMs is relatively high at small

Optics EXPRESS

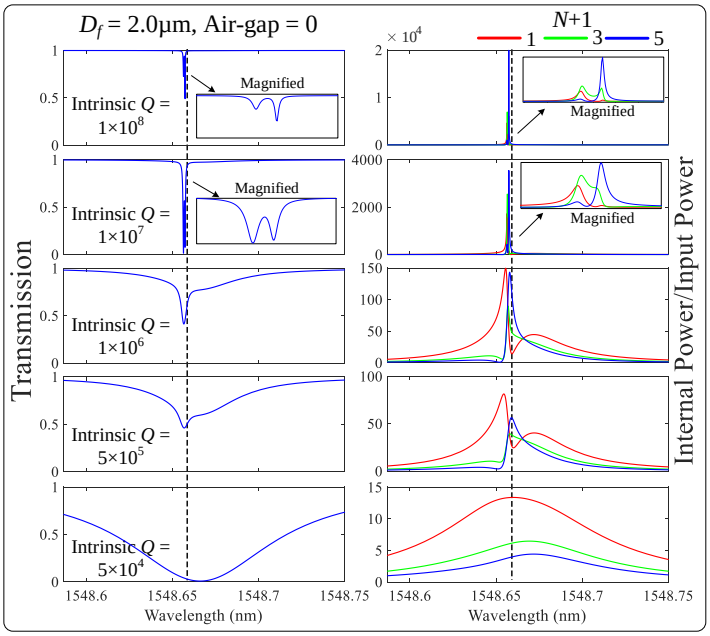

Fig. 4. Transmission and internal/input power spectra of the taper-coupled microsphere at zero air-gap and fixed taper diameter of 2μm when the intrinsic Q of the modes varies from 5×10^4 to 10^8 (insets show magnified view of the results for higher Q's)

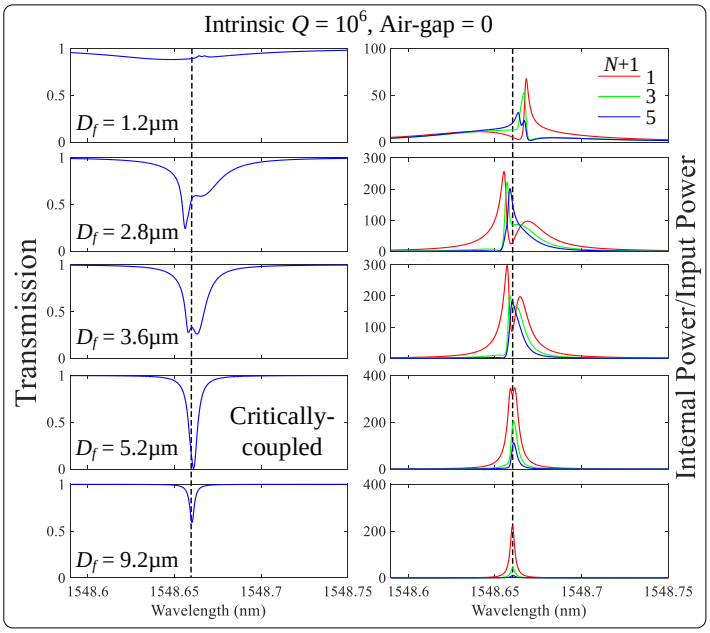

Fig. 5. Transmission and internal/input power spectra of the taper-coupled microsphere at zero air-gap and fixed intrinsic Q of 10^6 when the taper diameter varies from 1.2μm to 9.2μm (dashed lines show the position of the isolated microsphere resonance wavelength).

taper diameters due to high coupling coefficients between WGMs and fiber-mode. As the taper diameter increases, the interaction between WGMs decreases and the distorted line-shape of the resonance transmission develops again into a well-defined Lorentzian shape. At very large taper diameters, the fundamental mode is dominantly excited due to its lower phase-mismatch to the

Optics EXPRESS

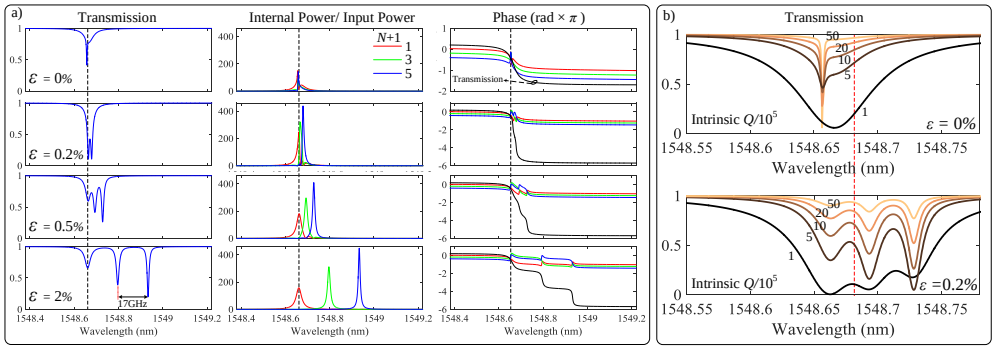

Fig. 6. a) Transmission, internal/input power and phase spectra of microsphere with a fixed intrinsic Q of 10^6 as a function of eccentricity showing various level of WGM interactions, and b) transmission spectra corresponding to eccentricities of zero and 0.2% as function of intrinsic Q factor (Q = 1, 5, 10, 20 and 50 $\times 10^5$), coupled to a tapered fiber at zero air-gap with diameter of 2μm (dashed lines show the position of the isolated perfect microsphere resonance wavelength).

fiber mode comparing to higher order WGMs. It is worth mentioning that, such tapered fibers with diameters of above 1.5μm are generally multimoded. Here, for the sake of simplicity in understanding the WGM interactions, we only consider the LP_{01} mode of the taper. It should be noted that, the amount of the modal overlaps and total Q's depend on the polarization of the taper and WGMs, as well. Thus, the regime under which WGMs operate will alter by changing the polarization state of the input light. Further experimental and theoretical studies on the polarization effects in microresonators are given in [20].

3.3. *Effects of microsphere eccentricity*

Experimental determination of degenerate WGMs is difficult, since any index perturbation on the cavity breaks the degeneracy, and WGMs shift in frequency depending on the strength of the perturbation and the order of the WGMs [21–24]. However, two or multiple WGMs, with different polarization states or radial orders, can be brought very close to each other in frequency, due to such perturbations. Therefore, simultaneous excitation of WGMs is common, especially in sizable microresonators which support larger number of modes (and exhibit smaller radiation losses). On the other hand, any deformation on a microsphere results in breaking the degeneracy of angular modes [25, 26]. In this regard, next, we use the developed CMT to further elucidate the effects of frequency degeneracy breaking on the transmission spectra of the taper-coupled microsphere resonators.

Frequency shift between the same radial order WGMs with consecutive angular orders is proportionally related to the amount of eccentricity defined by $\varepsilon = 1 - R_{minor}/R_{major}$ where R_{minor} and R_{major} respectively signify the length of the minor and major axes in a spheroid. Frequency shift ($\Delta\nu$) between pairs of WGMs for the group of angular modes studied here, considering an oblate spheroid with $R_{minor} = 30\mu m$, as a function of eccentricity, is calculated (from theory given in [26]) to be $\Delta\nu = 435\varepsilon$(GHz). Figure 6(a) plots the simulation results for eccentricities of 0, 0.5 and 2 percent. As previously discussed, when degenerate modes (i.e. $\varepsilon = 0\%$) are excited, modal interference distorts the transmission and internal power spectra from their Lorentzian line-shape. As a small eccentricity is introduced to the microsphere, WGMs are split in spectra varying the amount of modal interactions between distinct modes. Further increasing the eccentricity, decreases the cross-coupling between WGMs. At $\varepsilon = 2\%$, independent modal operation is enabled. The amount of WGM interactions is manifested in the phase spectra such that, slight eccentricity-induced-frequency-shift between modes, significantly lowers the effect of the cross-coupling on each mode's phase change. Thereby, absolute value

Optics EXPRESS

phase of the total transmission spectra is monotonically built-up ($\sim 2\pi$ per mode).

Note that, as an example, 0.5% eccentricity for a microsphere with 30μm radius implies a difference of about 150nm between major and minor radii. For bigger microspheres, the sensitivity of frequency degeneracy breaking to structural deformations is smaller. Nevertheless, small frequency shifts can be produced due to index perturbations by submicron sized particles [22]. Figure 6(b) shows the sensitivity of modal interference and the amount of visibility of frequency splitting as a function of Q factor for perfect (i.e. $\varepsilon = 0\%$) and slightly-eccentric (i.e. $\varepsilon = 0.2\%$) microspheres. As previously stated, at relatively small Q's ($Q = 10^5$), the modal interference is not strong enough due to low internal power of the modes. Hence, a perfect microsphere does not exhibit strong deterioration in its transmission spectra compared to a Lorentzian line-shape. Deformed microsphere, on the other hand, shows small ripples in the transmission owing to close resonances with low total Q's. As the Q factor increases, a perfect sphere shows strong modal interference, while, the deformed one maintains well-defined split resonances. Of course, the strength of WGM excitation depends on the coupling condition under which a mode is excited/collected. Such well-defined and clear single mode operation is important in CQED applications where interaction of a single atom with a single optical mode (preferably the fundamental one due to its high surface intensity) is desired. Interestingly, the eccentricity of a microsphere is shown to be controllably set by applying CO_2 laser pulses to a perfect microsphere without Q degradation [27, 28]. Alternatively, transition between perfect and deformed microspheres with various levels of deformations can be dynamically achieved by applying mechanical strain [29–31] to realize non-permanent deformations.

4. Conclusion

In this Paper, a general model based on CMT is developed to model multimode waveguides coupled to multimode cavities. Simulations show that excited coherent WGMs in a cavity are actually cross-coupled through the in-/output-coupling mechanism. The strength of the cross-coupling increases by the intrinsic Q factor of the WGMs, lowering the taper-resonator air-gap and decreasing the taper diameter. Such cross-coupling can transform the Lorentzian transmission spectrum to a Fano-like one. Moreover, the cross-coupling strength depends on the frequency coherence of the WGMs such that, depending on the total Q, a small frequency shift can decouple the effects of the WGMs on the transmission spectra. Note that our simulations are performed for the fundamental taper mode as the input and output mode of the system. However, in practice, such tapered fibers are multimoded, and WGMs can couple-out to different fiber modes depending on the resonance type and taper size (as we demonstrated in [32]). Furthermore, our study can be very useful in studying multimode cavities in nonlinear optics and lasers [33] where accurate determination of the internal intensity is important.

Funding

The Engineering and Physical Sciences Research Council (EPSRC) (EP/H02607X/1).

References

1. J. Ward and O. Benson, "WGM microresonators: sensing, lasing and fundamental optics with microspheres," Laser Photon. Rev. **5**, 553–570 (2011).
2. A. Chiasera, Y. Dumeige, P. Feron, M. Ferrari, Y. Jestin, G. Nunzi Conti, S. Pelli, S. Soria, and G. C. Righini, "Spherical whispering-gallery-mode microresonators," Laser Photon. Rev. **4**, 457–482 (2010).
3. M. R. Foreman, J. D. Swaim, and F. Vollmer, "Whispering gallery mode sensors," Adv. Opt. Photonics **7**, 168–240 (2015).
4. D. V. Strekalov, C. Marquardt, A. B. Matsko, H. G. Schwefel, and G. Leuchs, "Nonlinear and quantum optics with whispering gallery resonators," J. Opt. **18**, 123002 (2016).
5. S. M. Spillane, T. J. Kippenberg, O. J. Painter, and K. J. Vahala, "Ideality in a fiber-taper-coupled microresonator system for application to cavity quantum electrodynamics," Phys. Rev. Lett. **91**, 043902 (2003).
6. X. Wu and L. Tong, "Optical microfibers and nanofibers," Nanophotonics **2**, 407–428 (2013).

Optics EXPRESS

7. T. X. Hoang, S. N. Nagelberg, M. Kolle, and G. Barbastathis, "Fano resonances from coupled whispering-gallery modes in photonic molecules," Opt. Express **25**, 13125–13144 (2017).
8. B.-B. Li, Y.-F. Xiao, C.-L. Zou, Y.-C. Liu, X.-F. Jiang, Y.-L. Chen, Y. Li, and Q. Gong, "Experimental observation of fano resonance in a single whispering-gallery microresonator," Appl. Phys. Lett. **98**, 021116 (2011).
9. Y.-C. Liu, B.-B. Li, and Y.-F. Xiao, "Electromagnetically induced transparency in optical microcavities," Nanophotonics **6**, 789–811 (2017).
10. Y. Wang, K. Zhang, S. Zhou, Y.-H. Wu, M.-B. Chi, and P. Hao, "Coupled-mode induced transparency in a bottle whispering-gallery-mode resonator," Opt. Lett. **41**, 1825–1828 (2016).
11. C. Shun-Lien, "Application of the strongly coupled-mode theory to integrated optical devices," IEEE J. Quantum Electron. **23**, 499–509 (1987).
12. C. Shun-Lien, "A coupled-mode theory for multiwaveguide systems satisfying the reciprocity theorem and power conservation," J. Lightwave Technol. **5**, 174–183 (1987).
13. B. E. Little, J.-P. Laine, and H. A. Haus, "Analytic theory of coupling from tapered fibers and half-blocks into microsphere resonators," J. Lightwave Technol. **17**, 704 (1999).
14. N. Dubreuil, J. C. Knight, D. K. Leventhal, V. Sandoghdar, J. Hare, and V. Lefevre, "Eroded monomode optical fiber for whispering-gallery mode excitation in fused-silica microspheres," Opt. Lett. **20**, 813–815 (1995).
15. M. A. Popovic, C. Manolatou, and M. R. Watts, "Coupling-induced resonance frequency shifts in coupled dielectric multi-cavity filters," Opt. Express **14**, 1208–1222 (2006).
16. Z. Guo, H. Quan, and S. Pau, "Near-field gap effects on small microcavity whispering-gallery mode resonators," J. Phys. D: Appl. Phys. **39**, 5133–5136 (2006).
17. M. Larsson, K. N. Dinyari, and H. Wang, "Composite optical microcavity of diamond nanopillar and silica microsphere," Nano Lett. **9**, 1447–1450 (2009).
18. B.-B. Li, Y.-F. Xiao, C.-L. Zou, X.-F. Jiang, Y.-C. Liu, F.-W. Sun, Y. Li, and Q. Gong, "Experimental controlling of fano resonance in indirectly coupled whispering-gallery microresonators," Appl. Phys. Lett. **100**, 021108 (2012).
19. J. Liao, X. Wu, L. Liu, and L. Xu, "Fano resonance and improved sensing performance in a spectral-simplified optofluidic micro-bubble resonator by introducing selective modal losses," Opt. Express **24**, 8574–8580 (2016).
20. M. N. Mohd Nasir, S. Bakhtiari Gorajoobi, G. Senthil Murugan, and M. N. Zervas, "Polarization effects in optical microresonators," J. Opt. Soc. Am. B **36**, 705–716 (2019).
21. L. Deych and J. Rubin, "Rayleigh scattering of whispering gallery modes of microspheres due to a single dipole scatterer," Phys. Rev. A **80**, 061805 (2009).
22. X. Yi, Y.-F. Xiao, Y.-C. Liu, B.-B. Li, Y.-L. Chen, Y. Li, and Q. Gong, "Multiple-rayleigh-scatterer-induced mode splitting in a high-Q whispering-gallery-mode microresonator," Phys. Rev. A **83**, 023803 (2011).
23. L. Chantada, N. I. Nikolaev, A. L. Ivanov, P. Borri, and W. Langbein, "Optical resonances in microcylinders: response to perturbations for biosensing," J. Opt. Soc. Am. B **25**, 1312–1321 (2008).
24. B. Min, L. Yang, and K. Vahala, "Perturbative analytic theory of an ultrahigh-Q toroidal microcavity," Phys. Rev. A **76**, 013823 (2007).
25. M. L. Gorodetsky and A. E. Fomin, "Geometrical theory of whispering-gallery modes," IEEE J. Sel. Top. Quantum Electron. **12**, 33–39 (2006).
26. M. Sumetsky, Y. Dulashko, and R. Windeler, "Super free spectral range tunable optical microbubble resonator," Opt. Lett. **35**, 1866–1868 (2010).
27. J.-M. Cui, C.-H. Dong, C.-L. Zou, F.-W. Sun, Y.-F. Xiao, Z.-F. Han, and G.-C. Guo, "Controlling deformation in a high quality factor silica microsphere toward single directional emission," Appl. Opt. **52**, 298–301 (2013).
28. Y.-F. Xiao, C.-H. Dong, Z.-F. Han, G.-C. Guo, and Y.-S. Park, "Directional escape from a high-Q deformed microsphere induced by short CO_2 laser pulses," Opt. Lett. **32**, 644–646 (2007).
29. V. S. Ilchenko, P. S. Volikov, V. L. Velichansky, F. Treussart, V. Lefevre-Seguin, J. M. Raimond, and S. Haroche, "Strain-tunable high-Q optical microsphere resonator," Opt. Commun. **145**, 86–90 (1998).
30. T. Ioppolo, M. Kozhevnikov, V. Stepaniuk, M. V. Otugen, and V. Sheverev, "Micro-optical force sensor concept based on whispering gallery mode resonators," Appl. Opt. **47**, 3009–3014 (2008).
31. H. P. Wagner, H. Schmitzer, J. Lutti, P. Borri, and W. Langbein, "Effects of uniaxial pressure on polar whispering gallery modes in microspheres," J. Appl. Phys. **113**, 243101 (2013).
32. M. N. Mohd Nasir, G. Senthil Murugan, and M. N. Zervas, "Spectral cleaning and output modal transformations in whispering-gallery-mode microresonators," J. Opt. Soc. Am. B **33**, 1963 (2016).
33. S. B. Gorajoobi, G. S. Murugan, and M. N. Zervas, "Design of rare-earth-doped microbottle lasers," Opt. Express **26**, 26339 (2018).